DISCRETIZATION SCHEMES FOR MACROSCOPIC TRANSPORT EQUATIONS ON NON-CARTESIAN COORDINATE SYSTEMS

M. Spevak
T. Grasser

Institute for Microelectronics, Technical University Vienna, Austria
E-mail: {spevak|grasser}@iue.tuwien.ac.at

KEYWORDS
Discretization schemes, transport models, coordinate systems.

ABSTRACT

We present discretization schemes for the Poisson equation, the isothermal drift-diffusion equations, and a generalized higher-order moment equation of the Boltzmann transport equation for general orthogonal coordinate systems like cylindrical and spherical systems. The use of orthogonal coordinate systems allows to reduce the dimension of the problem from three to two. We give an approximation of the error which is made by using linear interpolation instead of the geometrically corrected interpolation.

INTRODUCTION

In order to solve the Poisson and the drift-diffusion equations finite differences or the method of finite volumes [1] are commonly applied. Due to a particular device design, for instance of short channel large width MOS transistors, it is often justified to assume that the electrical behavior is independent of the third coordinate. Thus, the problem can be reduced to two dimensions in a straightforward way. The same principle can be applied to other separable orthogonal coordinate systems. However, to the best of our knowledge, only rotationally symmetric cylindrical coordinate systems have been used so far in the context of semiconductor device simulation.
The simulation tool TRINE [2] introduces geometry adaptions for the method of finite volumes in order to simulate rotationally symmetric opto-electronic devices. This approach is limited to orthogonal grids and results in algebraically different formulae than the Scharfetter-Gummel scheme.
Commercial simulators like Dessis [3] and Medici [4] include cylindrical coordinate system capabilities, without going into details on the implementation. However, we could see that in some simulations the resulting values do not differ much from ours but are numerically not identical. This however can have several reasons such as different linear and nonlinear solver algorithms and slightly different model parameters.
If the material parameters and boundary conditions are independent of a coordinate it is possible to simplify the problem by elimination. One such case is found in rotationally symmetric cylindrical structures, which can easily be described in polar cylindrical coordinates exploiting their rotational symmetry because of the independence in respect to the azimuthal angle φ. The various issues regarding discretization schemes for general coordinate systems will be thoroughly investigated in the following.

EQUATION TYPES AND METRICS

We will discuss the equation system consisting of the Poisson equation, a generalized higher-order flux equation and the associated balance equation which read [5]:

$$\begin{aligned} \nabla \cdot \left(\underset{\sim}{\varepsilon}\, \nabla\psi\right) &= \varrho \,, \\ \mathbf{J}^k &= A^k \Big(\nabla\left(\xi^k\, T^k\right) - L^k\, \xi^k\, \nabla\psi \Big) \,, \\ \nabla \cdot \mathbf{J}^k &= \partial_t \xi^k + \nabla\psi \cdot \mathbf{J}^{k-1} + \xi^k \frac{T^k - T^k_{\mathrm{eq}}}{\tau^k} \,. \end{aligned} \tag{1}$$

Here $\underset{\sim}{\varepsilon}$ denotes the electric permittivity tensor, ψ is the electrostatic potential and ϱ is the charge density. The components of $\mathbf{J}^k$ denote the higher order fluxes [5]. τ^k denotes the relaxation time constant for the densities ξ^k which are associated with the fluxes $\mathbf{J}^k$. T^k is the carrier temperature and T^k_{eq} denotes the equilibrium temperature. A^k as well as L^k are matrial specific parameters.
In the following the three dimensional problem shall be reduced to two dimensions. The method of dimension reduction can be applied if several conditions are fulfilled. First all potential values have to be invariant with respect to the coordinate of separation. Therefore the gradient of these values must not point into the direction of separation. This means that the electric field as well as the fluxes of the higher-order moments have vanishing coefficients in the separated direction. If we have source terms such as charge and material parameters which are also independent from the separated coordinate we can assume the whole system totally independent from the coordinate.

After the separation of the invariant coordinate x_3 we have reduced the original three dimensional problem to two dimensions. Now the edges which connect two neighboring points have to be considered. Note that edges are affine under the back transformation Θ, for instance an iso-coordinate line for orthogonal grids. In general, however, these edges are not iso-coordinate lines. To facilitate the solution of the differential equations on these edges, a rotated coordinate system is introduced which guarantees that each edge can be described by a longitudinal and a normal component w and u (see Fig. 1).

$$x_1 = w\cos\alpha - u\sin\alpha \tag{2}$$
$$x_2 = w\sin\alpha + u\cos\alpha \tag{3}$$

We generalize the box integration method [1] for unstructured meshes based on Non-Cartesian metrics. For the gradient and the Laplace operator we get [6]

$$\begin{aligned}
\nabla f &= \mathbf{e}_w \partial_w f \Big(\frac{\cos^2\alpha}{g_1} + \frac{\sin^2\alpha}{g_2}\Big) ,\\
\nabla^2 f &= \frac{1}{h_1\, h_2\, h_3}\Big(\cos^2\alpha\ \partial_w\big(h_1 f'\big) + \sin^2\alpha\ \partial_w\big(h_2 f'\big)\Big) ,\\
f' &= \partial_w f\ , \qquad h_n = \frac{\prod_{j=1}^{3} g_j}{g_n^2}\ .
\end{aligned} \tag{4}$$

Here, g_n are the diagonal elements of the covariant metric tensor. They can be calculated by the following formula where $\mathbf{r}$ denotes the vector of position.

$$g_{ij}^2 = \partial_{x_i}\mathbf{r}\cdot\partial_{x_j}\mathbf{r}\ . \tag{5}$$

POISSON EQUATION

In the following section we will derive discretization schemes for the Poisson equation based on the method of finite volumes. The local flux density of the Poisson equation is the dielectric displacement which depends on the gradient of the potential. It is derived at the middle of the edge by the center point values of the electrostatic potential ψ. As we interpolate the electrostatic potential on a mesh edge we can thus calculate the displacement.

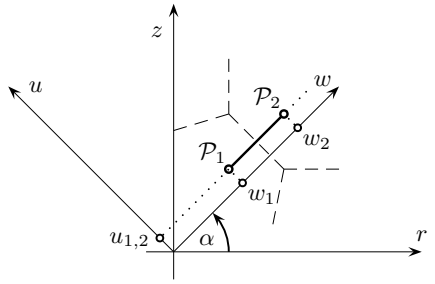

Figure 1: An arbitrary connection line between two vertices $\mathcal{P}_1$ and $\mathcal{P}_2$ of the Delauney triangulation. With respect to the geometric points we introduce a coordinate system on the coordinates u and w so that the connection edge is an iso-coordinate line with respect to u. α denotes the skew angle. In dashed lines we can see a part of the Voronoi diagram.

In the finite volume method the source terms are moved to the center points of the finite volumes. Thus no sources are located at the edges and we can derive the potential distribution solving the homogeneous equation $\nabla\cdot\big(\underline{\varepsilon}\cdot\nabla\psi\big) = 0$. The electric field which is calculated in the middle between two neighboring volume centers is obtained from the projection of the field strength onto the normalized edge direction vector $\mathbf{n}$. We thus obtain

$$\frac{1}{h_1 h_2 h_3}\Big(\partial_{x_1}\big(h_1\partial_{x_1}\psi\big) + \partial_{x_2}\big(h_2\partial_{x_2}\psi\big)\Big) = 0\ . \tag{6}$$

Even though the Poisson equation is assumed to be isotropic in the following sections the extension to anisotropic media is straightforward. However, the solution of the total equation system can only be rotationally symmetric if the material tensors fulfill the following conditions: all tensor components with the separated coordinate except the diagonal element g_3 have to vanish and, in addition, the tensor components must not depend on the separated coordinate x_3.

Under the assumption of rotational or translational symmetry the discretized Poisson equation becomes

$$\begin{aligned}
\varrho_i V_i &= \sum_{j=1}^{n} \underline{\varepsilon}\,\nabla\psi\big|_{ij} A_{ij}\ ,\\
\nabla\psi &= G\Delta\psi\frac{H}{\int_{w_i}^{w_j} H\,\mathrm{d}w'}\ ,\\
H\big(w\big) &= \Big(\cos^2\alpha\, h_1 + \sin^2\alpha\, h_2\Big)^{-1}\ ,\\
G\big(w\big) &= \frac{\cos^2\alpha}{g_1} + \frac{\sin^2\alpha}{g_2}\ .
\end{aligned} \tag{7}$$

The surfaces A_{ij} and box volumes V_i can be calculated by a straightforward extension of the Guldin rules for cylindrical coordinates. For other coordinate systems they can be numerically evaluated. To quantify the deviation from the Cartesian case we define a geometry factor $\mathcal{G}$ as the ratio between the general coordinate and Cartesian coordinate discretization of the flux. In the case of the Poisson equation the geometry factor is proportional to the gradient operator. For cylindrical coordinates we obtain for the gradient

$$\nabla\psi\Big|_{\overline{r_\mathrm{a}}}^{\mathrm{cyl}} = \frac{\Delta\psi}{\Delta w}\,\frac{\overline{r_\mathrm{l}}}{\overline{r_\mathrm{a}}}\ , \qquad \mathcal{G}_\mathrm{P}^{\mathrm{cyl}} = \frac{\overline{r_\mathrm{l}}}{\overline{r_\mathrm{a}}}\ ,$$

with $\overline{x_\mathrm{l}} = \big(x_i - x_j\big)/\ln\big(x_i/x_j\big)$ and $\overline{x_\mathrm{a}} = \big(x_i + x_j\big)/2$. This is equivalent to the result obtained in [2].

TRANSPORT EQUATIONS

The transport equations are more complicated to handle. First, the isothermal drift-diffusion equations are

considered because the solution of the resulting ODE can be written explicitly in terms of integrals. With $T = \text{const}$ we obtain a current discretization which is akin to the well known Scharfetter-Gummel scheme [7]. The solution of the Poisson equation is inserted into the flux relation so as to obtain a consistent discretization for the potential. Generally, this leads to an integral formulation which cannot be evaluated analytically and therefore closed form solutions do not exist for every coordinate system. However, for some important coordinate systems analytic solutions exist. For instance, for cylindrical coordinates one obtains

$$J_w^{\text{cyl}} = \frac{A\,T}{\Delta w}\frac{\overline{r_{\text{l}}}}{\overline{r_{\text{a}}}}\Big(\xi_i^k \mathcal{B}\big(\Lambda\big) - \xi_j^k \mathcal{B}\big(-\Lambda\big)\Big) = \\ = \frac{\overline{r_{\text{l}}}}{\overline{r_{\text{a}}}} J_w^{\text{cart}} = \mathcal{G}_{\text{DD}}^{\text{cyl}} J_w^{\text{cart}}\,. \tag{8}$$

The $\overline{r_{\text{a}}}$ and $\overline{r_{\text{l}}}$ denote the arithmetic and the logarithmic mean of the radii of $\mathcal{P}_1$ and $\mathcal{P}_2$. Note that the geometry factors for the Poisson equation and the isothermal drift-diffusion equations are the same for cylindrical coordinates. This is not the case for arbitrary coordinate systems. In [2] a linear potential interpolation between the mesh points was proposed which, however, leads to elliptic integrals for cylindrical coordinates.

For higher-order moment equations or the non-isothermal drift diffusion equations no exact solution can be given [5]. Conventionally, the temperature is assumed to vary linearly between the mesh points [5]. For the generalization to Non-Cartesian coordinates we note that similarly to the Poisson equation, the temperature flux between the mesh points is free of divergence. Because of the fact that the homogeneous stationary equations for the temperature have the same structure we obtain the same interpolation for T as for the potential. To solve the inhomogeneous first order equation the optimum artificial diffusivity method [5] is generalized to Non-Cartesian coordinates and we obtain

$$J_w = J_w^{\text{cyl}} = \frac{A\,\overline{T}_{\text{l}}}{\Delta w}\Big(\xi_j^k \mathcal{B}\big(\Lambda\big) - \xi_i^k \mathcal{B}\big(-\Lambda\big)\Big)\,, \\ \Lambda = \frac{\big(\Delta T - L\Delta\psi\big)}{\overline{T_{\text{l}}}}\,. \tag{9}$$

No geometry factor appears due to the averaging procedure employed in the generalized optimum artificial diffusivity method. The scheme (9) does therefore not reduce to (8) for $T = \text{const}$. The Non-Cartesian geometry only enters the discretized balance equations through A_{ij} and V_i and we obtain [8]

$$\sum_{j=1}^{N} A_{ij} J_w^k - V_i \frac{\xi_{t-\Delta t}^k - \xi_t^k}{\Delta t} + \sum_{j=1}^{N}\big(\psi_j - \psi_i\big) A_{ij}\, J_w^{k-1} - \\ - V_i\, \xi^k\, \frac{T^k - T_{\text{eq}}^k}{\tau^k} = 0\,.$$

For the isothermal drift-diffusion model a geometry factor has been introduced in (9) which is the ratio of linear interpolation and geometry adapted interpolation. For cylindrical coordinates the geometry factor can be expressed as the ratio between two different mean values of the same quantity. The discretization of the isothermal drift-diffusion model with the generalized optimum artificial diffusivity method, however, gives 1 instead of $\overline{r_{\text{l}}}/\overline{r_{\text{a}}}$ as geometry factor. Assuming a maximum change of size of neighboring elements of 1.61, as suggested by the Golden Section, we obtain a geometry factor of 0.97.

BOUNDARY CONDITIONS

For the sake of completeness we have to introduce the boundary conditions. The boundary conditions for the potential are of Dirichlet or Neumann type and read

$$\partial_{\mathbf{n}}\Psi = 0 \qquad \Psi = f\big(\mathbf{r}\big)\,. \tag{10}$$

For the higher-order moment equations we use

$$\xi^{(k)} = n_{\text{c}}\, T_{\text{L}}^k\,, \qquad T_{\text{F}}^{(k)} = T_{\text{L}}. \tag{11}$$

All Zero-Neumann as well as Dirichlet boundary conditions can be handeled implicitly in finite volumes and do not need any further discretization. These boundary conditions are pre-eliminated in the final equation system.

ERROR APPROXIMATION

Due to the introduction of the geometry factor $\mathcal{G}$ the resulting system matrix of the Poisson equation as well as the continuity equation are slightly changed. Because the inhomogeneity of the partial differential equations is not influenced by the geometry dependent interpolation scheme, only the influence on the matrix will be considered in the following basic analysis, based on a one-dimensional simulation domain. To estimate the influence of the geometry factors on the final result a new system matrix is written as the sum of the original matrix and an incremental matrix:

$$\mathbf{A}_{\mathcal{G}} = \mathbf{A} + \Delta\mathbf{A}_{\mathcal{G}}\,. \tag{12}$$

The original matrix can be written as

$$\mathbf{A} = \begin{bmatrix} -1-a_1 & a_1 & 0 & 0 \\ 1 & -1-a_2 & a_2 & 0 \\ 0 & 1 & -1-a_3 & a_3 \\ 0 & 0 & \ddots & \ddots \end{bmatrix}, \tag{13}$$

$$a_i = \frac{A_i/d_i}{A_{i+1}/d_{i+1}}\,. \tag{14}$$

whereas the final matrix looks like the following 15. Note that we had to make a base transformation in order to obtain unity for each sub-diagonal entry.

The main diagonal elements of the original matrix $\mathbf{A}$ are multiplied with factors which are derived from the

geometry factor, $\gamma_i = 1 - \mathcal{G}_i/\mathcal{G}_{i+1}$. Therefore we retrieve the modified matrix

$$\Delta\mathbf{A}_{\mathcal{G}} = \begin{bmatrix} \gamma_1 a_1 & -\gamma_1 a_1 & 0 & 0 \\ 0 & \gamma_2 a_2 & -\gamma_2 a_2 & 0 \\ 0 & 0 & \gamma_3 a_3 & -\gamma_3 a_3 \\ 0 & 0 & \ddots & \ddots \end{bmatrix} , \quad (15)$$

$$\gamma_i = 1 - \frac{\mathcal{G}_i}{\mathcal{G}_{i+1}} . \quad (16)$$

An a priori deviation of the solution of the linear equation system is found to be:

$$\frac{\|\Delta\mathbf{x}\|}{\|\mathbf{x}\|} \leq \frac{\max_i \gamma_i a_i}{1 - \max_i \gamma_i a_i} \leq \frac{\gamma_{\max} a_{\max}}{1 - \gamma_{\max} a_{\max}} . \quad (17)$$

In typical simulations the maximal geometry dependent term γ_2 is about $1 - 10^{-3}$ to $1 - 10^{-4}$. As a consequence typical relative deviations in current and charge are only about 10^{-3}. This suggests that for relevant simulations this geometry factor has little effect on the result.
In order to support this theory that the deviation has no effect it is shown that the deviation is of higher order than the discretization error. The geometry factors as well as the box distances and surfaces are expressed in terms of h, the radial distance between two mesh points. For the calculation of the factors we use three points in a radial line with the radii r, $r - h_{12}$ and $r - h_{23}$. The box surfaces and distances go with $O(h^2)$ and $O(h)$, respectively. The geometry factors for the interpolation correction between the points is then obtained as

$$\mathcal{G}_{12} = \frac{h_{12}}{(r - h_{12}/2)\ln\big((r - h_{12})/r\big)} ,$$
$$\mathcal{G}_{23} = \frac{h_{23}}{(r + h_{23}/2)\ln\big((r + h_{23})/r\big)} , \quad (18)$$

where it is assumed that h_{12} and h_{23} are either equal (uniform grid) or of the same order of magnitude (quasi-uniform grid).
The deviation matrix $\Delta\mathbf{A}_{\mathcal{G}}$ is determined by γ_2 which reads for uniform grids

$$\gamma_2 = 1 - \frac{\mathcal{G}_{23}}{\mathcal{G}_{12}} = -\frac{h^3}{6\,r^3} + O\big(h^4\big) . \quad (19)$$

From the Taylor expansion of (19) we obtain the h dependence of the resulting deviation. After some basic calculations one finds an $O(h^3)$ dependence for uniform grids and an $O(h^2)$ dependence for quasi-uniform grids. The method of finite volumes as well as the finite difference method lead to numerical errors going with $O(h^2)$ for uniform grids and $O(h)$ for quasi uniform grids [1]. Thus, if the grid is refined the numerical error will always be larger than the deviation caused by the geometry factor. Therefore the use of a properly designed grid seems to be sufficient to keep the influence of the geometry corrected interpolation smaller than the general discretization error.

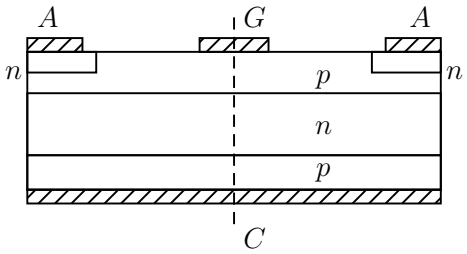

Figure 2: Rotationally symmetric thyristor

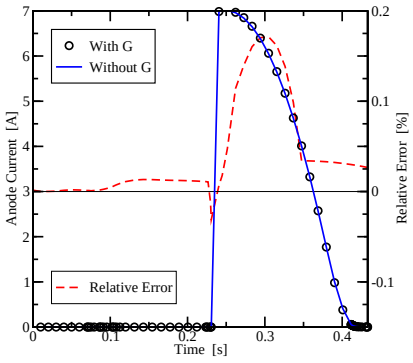

Figure 3: Rotationally symmetric thyristor ignition characteristics.

RESULTS

The second example shows a rotationally symmetric thyristor (see Fig. 2) with *n-p-n-p* doping levels of $10^{19}\,\mathrm{cm}^{-3}, 10^{17}\,\mathrm{cm}^{-3}, 10^{17}\,\mathrm{cm}^{-3}$, and $10^{19}\,\mathrm{cm}^{-3}$. The device radius is $8\,\mu$m, the device thickness is $5\,\mu$m. We simulate the ignition of the thyristor by applying a voltage pulse of 0.5 V to the gate with a constant applied anode voltage of 2 V. As shown in Fig. 3 we obtain a current of 7 A and a typical difference between the geometry-corrected and the standard discretization of about 10^{-3}, which further demonstrates the correctness of our initial assumption.
Figure 3 shows this thyristor ignition obtained from the two dimensional simulation conducted by Minimos-NT [9] using the cylindrical and Cartesian discretisation.
The geometry of the investigated FET is shown in Fig. 4. We assume doping levels of $2 \times 10^{20}\,\mathrm{cm}^{-3}$ in the source and drain regions, an intrinsic channel region, an oxide thickness of 1 nm, and a channel length of 50 nm.

CONCLUSION

A method of reducing the dimensionality of a given problem has been presented for Non-Cartesian coor-

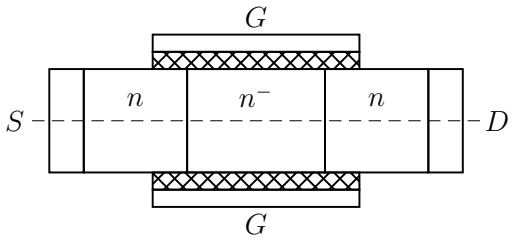

Figure 4: Surrounding gate FET

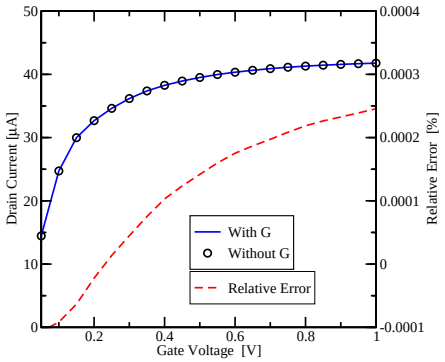

Figure 5: Surrounding gate FET output characteristics.

dinate systems. The proposed method can also easily be applied to other coordinate systems, like for instance spherical coordinates and elliptic cylindrical coordinates, both for rotational and translational symmetry. In the most general case, the geometry factors have to be determined by numerical integration and their influence on the final result has to be assessed.

Based on the results obtained so far, however, we can state that at least for cylindrical coordinates, which are most the relevent Non-Cartesian coordinate systems, the error caused by a linear interpolation scheme is of higher order than the discretization error and therefore can be neglected.

It has been shown that for cylindrical coordinates it is sufficient to account for the modified geometry by modified box volumes and surfaces while pertaining the same flux discretization as used for Cartesian grids.

REFERENCES

[1] S. Selberherr, *Analysis and Simulation of Semiconductor Devices* (Springer, Wien–New York, 1984).

[2] K. Matsumoto, I. Takayanagi, T. Nakamura, and R. Ohta, **38**, (1991).

[3] *DESSIS-ISE, ISE TCAD Release 9.5*, ISE Integrated Systems Engineering AG, Zürich, Switzerland, 2004.

[4] *Medici, Two-Dimensional Device Simulation Program, Version 2002.4*, Synopsys Corporation, Mountain View, CA, 2003.

[5] T. Tang and M.-K. Ieong, IEEE Trans.Computer-Aided Design **14**, 1309 (1995).

[6] W. Neutsch, *Koordinaten* (Spektrum Akademischer Verlag, 1995).

[7] D. Scharfetter and H. Gummel, IEEE Trans.Electron Devices **16**, 64 (1969).

[8] T. Grasser, H. Kosina, M. Gritsch, and S. Selberherr, J.Appl.Phys. **90**, 2389 (2001).

[9] IμE, *MINIMOS-NT 2.1 User's Guide*, Institut für Mikroelektronik, Technische Universität Wien, Austria, 2004, http://www.iue.tuwien.ac.at/software/minimos-nt.

BIOGRAPHIES

MICHAEL SPEVAK studied electrical engineering at the TU Wien. He joined the Institute for Microelectronics in December 2004, where he is currently working on his doctoral degree.

TIBOR GRASSER is currently employed as an Associate Professor at the Institute for Microelectronics. In 2003 he was appointed head of the Christian Doppler Laboratory for TCAD in Microelectronics, an industry-funded research group embedded in the Institute for Microelectronics. His current scientific interests include circuit and device simulation and device modeling.